

# Registering 3D Objects Triangular Meshes using An Interest Point Feature Extraction on Barycentric Coordinates

Tibyani Tibyani

Information Architecture Field

Graduate School of Information,

Production and System, Waseda University

2-7 Hibikino, Wakamatsu, Kitakyushu,

Fukuoka 808-0135, Japan

Email: tibyani@akane.waseda.jp

Sei-ichiro Kamata

Information Architecture Field

Graduate School of Information,

Production and System, Waseda University

2-7 Hibikino, Wakamatsu, Kitakyushu,

Fukuoka 808-0135, Japan

Email: kam@waseda.jp

**Abstract**—In this paper, an interest points feature extraction algorithm is proposed to extract salient local features from 3D object models and combine with a spin algorithm to register them. A framework is presented in this study. This method make use of 3D Harris-Laplacian Detector method of feature points in barycentric coordinate. Using this approach, we can extract the object correctly and robustly in noise situation. The unique advantage of this framework is its applicability to triangular mesh models. Experimental results on a different number of models are shown to produce the effectiveness and robustness of our framework of feature extraction approach and demonstrate more accurate results for global registering 3D object models for three pairs of corresponding *interest points* features.

## I. INTRODUCTION

As surface acquisition 3D range images are becoming more popular and widely used for the three-dimensional geometric data in many applications of geometric modeling, computer graphics and computer vision, such as 3D object registration, feature detection, discrete surface segmentation, rendering and shape recovery.

In 3D object registration, such features are usually local around a point in the sense that for a given point in the scene its closeness is used to determine the corresponding feature. This task consists of two major phases, namely the identification of appropriate points, often referred to as *interest points*, *feature points*, *salient points* or *key points* and the way in which the information in the near of that point is encoded in a descriptor or description vector. They are those points which are distinctive in their locality. ([1]–[3],[5]–[7],[9],[14],[17],[22]). Important advantages of *interest points* are that they substantially reduce the search space and computation time required for finding correspondences between models to scenes and that they furthermore focus the computation on areas that likely relevant for the registration and matching processes. There has been surprisingly little research for *interest points* extraction in raw 3D modeling data in the past, compared to vision, where this is a well researched area.

In this paper we present the *interest points* extraction method together with a feature descriptor for points in 3D range data through scale space 3D Harris-Laplacian Detector, local covariance computation, PCA (Principal Component Analysis) and Barycentric. The outer forms are often rather unique so that their explicit use in the interest point extraction and the descriptor calculation can be expected to make the overall process more robust.

The main contribution of this paper is to propose a 3D object *interest points* feature extraction algorithm based barycentric coordinates. This framework gives a unique and viewpoint-independent description of a local shape. We introduce a method for *interest points* extracting the local features from 3D triangular meshes data. The proposed approach is applied on a variety of 3D models with different noise levels to demonstrate its robustness and effectiveness and combined with a spin image algorithm to register 3D surfaces.

Spin images have been particularly successful to be a powerful method for object matching because they are translation, rotation, scale and pose invariant. Johnson and Hebert experimented spin images to reduce the dimensionality of spin images and use closest point search to reduce the time required for matching [1]. Other extensions of this method including the multi-resolution and interpolating [26],[27], large and sampling 3D datasets [24],[25], reducing high computational cost [28],[29] and scaling [30]. However, the main demerit of the spin images representation is that it has a low discriminating capability and thus, may lead to many equivocal correspondences.

The rest of this paper is organized as follows. In Section 2, we describe a fundamental of barycentric coordinates theory. In Section 3, we briefly describe spin images. In section 4 we describe pairwise registration. In section 5 we construct *Interest points* Feature Detection Using scale space Harris-Laplacian Detector algorithm. In Section 6, we give detail of algorithm registering from 3D object model in Section 7, present our experiments and results along with their quan-

tative analysis. In Section 8, we give our conclusions and directions for future work.

## II. BARYCENTRIC COORDINATES

A triangle is given by three points,  $p_1$ ,  $p_2$  and  $p_3$ , its vertices. The vertices may live in 2D or 3D. Three points define a plane, therefore, a triangle is a 2D element. For the following development, the triangle is given in the xy-plane ([16],[20],[21]). A barycentric combination of three points is given by

$$p = up_1 + vp_2 + wp_3 \quad (1)$$

where,  $u + v + w = 1$  Therefore,  $p$  embeds in this plane, and we say  $[u, v, w]$  are the barycentric coordinates of  $p$  with respect to  $p_1$ ,  $p_2$  and  $p_3$ , respectively. Equivalently, we may define, then

$$p = up_1 + vp_2 + (1 - u - v)p_3 \quad (2)$$

The Equation (1) represents three equations, and thus we can form a linear system, The system of equations can be written in matrix terms as

$$\begin{pmatrix} p_1 & p_2 & p_3 \\ 1 & 1 & 1 \end{pmatrix} \begin{pmatrix} u \\ v \\ w \end{pmatrix} = \begin{pmatrix} p \\ 1 \end{pmatrix} \quad (3)$$

for the unknown  $u, v, w$ . To solve this system using Cramer's rule as in [15] and recall that determinants correspond to signed areas :

$$\begin{vmatrix} p_1 & p_2 & p_3 \\ 1 & 1 & 1 \end{vmatrix} = A \quad (4)$$

$$\begin{vmatrix} p & p_2 & p_3 \\ 1 & 1 & 1 \end{vmatrix} = A_1 \quad (5)$$

$$\begin{vmatrix} p_1 & p & p_3 \\ 1 & 1 & 1 \end{vmatrix} = A_2 \quad (6)$$

$$\begin{vmatrix} p_1 & p_2 & p \\ 1 & 1 & 1 \end{vmatrix} = A_3 \quad (7)$$

Therefore,

$$u = A_1/A, v = A_2/A, w = A_3/A \quad (8)$$

$p_1 \cong [1, 0, 0]$ ,  $p_2 \cong [0, 1, 0]$  and  $p_3 \cong [0, 0, 1]$ .

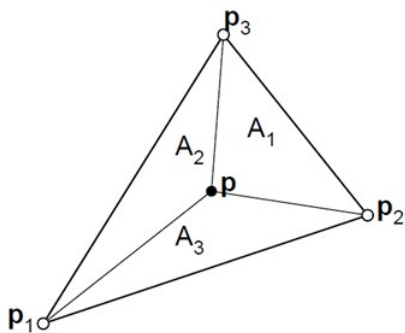


Fig. 1. The barycentric coordinates of a point  $p$  with respect to a triangle are defined in terms of ratios of triangle areas[21]

## III. REGISTRATION USING SPIN IMAGES

Spin images (SI) were introduced in the seminal work of a feature description method to characterize the properties of 3D object with respect to a single oriented point. It is a surface representation that uses 2D images to describe 3-D oriented points. Each spin-image is a local surface descriptor calculated at an oriented point  $(p, n)$  (3D point with normal vector) by encoding two of the three cylindrical coordinates of the its surrounding points(Fig. 2). The spin-image  $X$  for a surface point  $p$  is a 2D histogram in which each pixel is a bin that stores the number of neighbours that are a distance  $a$  from  $n$  and a depth  $b$  from its tangent plane  $P$ . More precisely, it is assumed that all the 3D data given as mesh triangular of 3D Objects  $Mesh = V, E$  where  $V$  are the vertices and  $E$  the edges. Lets consider a vertex  $P \in V$ . The spin image axis are the normal to the point  $P$ , and a perpendicular vector to this normal. The former one is called  $\beta$  and the latter one  $\alpha$ . The support region of a spin image is a cylinder centred on  $P$ , and aligned around its normal. From this, each point of the model is assigned to a ring with a height along  $\beta$ , and a radius along  $\alpha$ . The similarity of two spin-images is measured by calculating their correlation coefficient. The registration of two different views are performed by finding the correspondences between points on the surfaces using the similarity of their spin-images. Correspondence pairs with highest similarity that are geometrically consistent are selected to estimate the rigid transformation that registers the surfaces. As the surface positions chosen to compute spin-images are selected randomly, this may reduce the accuracy of the registration as a result of missing important geometric structures. By incorporating our feature selection framework into the spin-image algorithm, we can improve not only its robustness by using *interest points* features in the matching process but also the accurate as the number of features is significantly smaller than the number of randomly selected points[1]. However, the pairwise registration method using spin images is only suitable to 3D objects meshes with information of connectivity Betwixt the vertices.

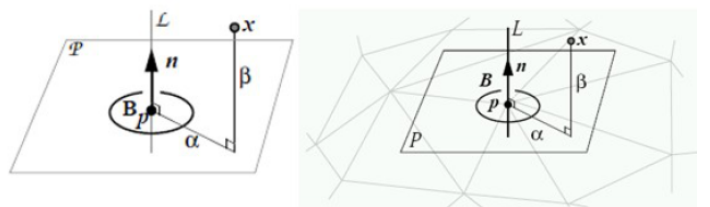


Fig. 2. An oriented point basis on planar and on mesh

## IV. PAIRWISE REGISTRATION

The registration of 3D datasets such as range images (or views) is performed pairwise and it can be divided in two steps. First, the views are coarsely registered and second, the 3D registration is refined with a fine registration algorithm. Any pair  $(r, s)$  of range images have set of correspondences  $C_{rs}$

$= \{ (i,j) \mid \mathbf{p}_i^r \in P^r \text{ and } \mathbf{p}_j^s \in P^s \text{ corresponding} \}$  where any range image r a set  $P^r$  of scale feature points  $\mathbf{p}_i^r$ . Coarse registration is furthered by a fine registration algorithm which iteratively refines the initial coarse registration. By finding the match that registers the largest number of interest point features between the two range images, the best transformation is able to be estimated. This transformation can be follow refined using a variant of the Iterative Closet Point(ICP) algorithm [23],[31]. To solve among the set of all rigid transformation using the solution to the local minimization problem  $T_{rs} = \text{argmin}_{T,r,s} \varepsilon(T,r,s)$  where the error of registration  $\varepsilon(r,s) = \sum_{(i,j) \in C_{rs}} d^2(\mathbf{p}_i^r, \mathbf{p}_j^s)$

## V. INTEREST POINTS FEATURE DETECTION USING SCALE-SPACE HARRIS-LAPLACIAN DETECTOR

The Harris corner and edge detector has been one of the most successful algorithms in detection [8]. Let  $x$  be a vertex of the shape  $X$  and  $V_k(x)$  denote the neighborhood of  $k$  rings around  $x$ . First, the centroid of  $V_k(x)$  is calculated, and the set of points is translated so the centroid is in the origin of the 3D coordinate system. Next, a plane is fit to the translated points applying PCA (Principal Component Analysis) to the set of points and choosing the eigenvector with the lowest associated eigenvalue as the normal of the fitting plane. The set of points is rotated so that the normal of the fitting plane is the z-axis. To calculate derivatives, a quadratic surface  $f(u,v)$  is fit to the set of transformed points. Second, the matrix E associated to the point  $x$ ([8],[18],[19]).

$$E = \begin{pmatrix} A & C \\ C & B \end{pmatrix} \quad (9)$$

$$A = \frac{1}{\sqrt{2\pi}\sigma} \int_R^2 e^{-\frac{(u^2+v^2)}{2\sigma^2}} f_u^2(u,v) du dv \quad (10)$$

$$B = \frac{1}{\sqrt{2\pi}\sigma} \int_R^2 e^{-\frac{(u^2+v^2)}{2\sigma^2}} f_v^2(u,v) du dv \quad (11)$$

$$C = \frac{1}{\sqrt{2\pi}\sigma} \int_R^2 e^{-\frac{(u^2+v^2)}{2\sigma^2}} f_u(u,v) f_v(u,v) du dv \quad (12)$$

And  $\sigma$  is parameter defining the support Gaussian function. The Harris operator value at point  $x$  is calculated as  $H(x) = \det(E) - 0.04(\text{tr}(E))^2$ . Then a constant fraction of the total number of vertices with the highest Harris operator response is selected as feature point([8],[9]). The Gaussian scale space representation can be created by convolving the image  $I(x)$  with Gaussian kernels  $G$  [22].  $L(x, scaling) = G(scaling) * I(x)$  with  $I$  the image and  $x = (x,y)$ . The scale normalized derivative D of order m is defined by,  $D_{i_1 \dots i_m}(x, scaling) = scaling^m L_{i_1 \dots i_m}(x, scaling) = scaling^m G_{i_1 \dots i_m}(scaling) * I(x)$ . Image derivatives are then related,  $scaling^m G_{i_1 \dots i_m}(scaling) * I(x) = t^m scaling^m G_{i_1 \dots i_m}(t, scaling) * I(x')$  for relation between the two images  $I(x) = I(x')$  where  $x' = t \cdot x$ . Thus, for normalized derivatives we obtain,

$$D_{i_1 \dots i_m}(x, scaling) = D_{i_1 \dots i_m}(x, t, scaling) \quad \text{Square gradient}$$

$$scaling^2(L_x^2(x, scaling) + L_y^2(x, scaling)) \quad (13)$$

Laplacian

$$|scaling^2(L_{xx}(x, scaling) + L_{yy}(x, scaling))| \quad (14)$$

Multi scale Harris function

$$\det(C) - \alpha \text{trace}^2(C) \quad (15)$$

with  $C(x, scaling, \bar{scaling}) = scaling^2 G(x, \bar{scaling}) * \begin{pmatrix} L_x^2(x, scaling) & L_x L_y(x, scaling) \\ L_x L_y(x, scaling) & L_y^2(x, scaling) \end{pmatrix}$  In these works, we use the multi scale Harris detector to detect interesting points at different resolution  $L(x, scaling_n)$ , with  $scaling_n = k^n scaling_0$ ,  $scaling_0$  is the initial scale factor [22].

## VI. REGISTERING FROM 3D OBJECT MODELS

The method we propose is to obtain and choose these *interest points* which carry the significant geometry information of the triangular meshes as the feature points and combine with a spin image algorithm to register 3D Object models. The overall steps are as follows :

1. Input 3D Data with vertex and face.
2. Calculate the centre of vertex  $v_k(x)$ .
3. Compute mesh triangular local covariance.
4. Compute Scale space Harris-Laplacian detection.
5. Translate the set of points to the centre in the origin of the 3D coordinate system.
6. Fit points to a plane applying PCA (Principal Component Analysis) and Barycentric Coordinate.
7. Choose the eigenvector with the lowest associated eigenvalue as the normal of the fitting plane.
8. Compute and declare *interest points*.
9. Spin images selection as surface descriptors and Finding pairs of matched.
10. Correspondence verification using a pruning algorithm[32].
11. Registering two views of 3D Object models with three pairs of corresponding features.

## VII. EXPERIMENTS AND RESULTS

The proposed a framework feature extraction approach was tested on a variety of standard 3D models. Figure and visualize the *interest points* extracted from 10 different 3D models. The 'Chef', 'Chicken', 'T-rex', 'Rhino' and 'Parasaurolophus' models could be downloaded from the Mian's web side as in [3] and [13]. The 'Dragon' and 'Buddha' models were found from the Stanford 3D Scanning Repository as in[12]. The 'Angel', 'Bigbird' and 'Zoe' models were taken from B. Taati Queen's Range Image and 3-D Model Database from Queen university web side as in [10] and [11]. It can be analyzed from the figures that most of the salient positions in the models such as locations close the noses, mouths or eyes of the Buddha and Chef, the tail of the Dragon or Chicken together with many others were selected as feature points.

The comparison between the number of *interest points* and the number of vertices in each model as shown in Table I. It can be depicted in the table that the number of *interest points* is significantly smaller than the number of vertices in all 10 surfaces. Feature points extraction from the Chicken and Angel

TABLE I  
COMPARISON BETWEEN THE NUMBER OF VERTICES AND NUMBER OF  
INTEREST POINTS FOR ALL 10 MODELS

Models	Number of Vertices	Interest Points
Dragon	134559	3929 (2.92 percent)
Rhino	79934	1287 (1.61 percent)
Zoe	5002	166 (3.31 percent)
Buddha	133127	2929 (2.22 percent)
Parasaurolophus	184933	3458 (1.87 percent)
T-rex	176508	2995 (1.70 percent)
Chicken	135142	2608 (1.93 percent)
Bigbird	5003	159 (3.17 percent)
Cheff	176920	2672 (1.51 percent)
Angel	4998	160 (3.14 percent)

view models for different levels of noise as shown Fig.3. It can be looked from the figure that a large portion of local points feature from original, smooth surface are described in the noisy versions. For example, there are still many feature points embedding around salient structures as nose, chin, lip, eyes, mouth and ear for Angel view model in Fig.3(h). For Chicken model, beak or pecker, cockscomb and crest are lied many the *interest points* features as shown Fig.3(d).

In order to evaluate the repeatability of the feature points, white Gaussian Noise with standard deviation  $\sigma$  is set at various values:  $\sigma = 0.05$ ,  $\sigma = 0.1$  and  $\sigma = 0.2$  for chicken and  $\sigma = 0.05$ ,  $\sigma = 0.1$  and  $\sigma = 0.2$  for Angel view. The impacts of noises on the surface Chef and Angel view models are shown in Fig.3. The results show that the variation of local surface patches will increase. Overall, there would be more features points detected in noisy images compared the original one.

The repeatability evaluation method that use in this work use as in [4]. A quantitative evaluation of the repeatability of the points features for 10 different 3D models is shown in Fig.5. At the level noise level  $\sigma = 0.05$  nearly all of the features in the original model can be detected in the noisy surface. Even when the standard deviation of the noise goes to  $\sigma = 0.2$ , about 0.51 of the original features repeat in the noisy data.

Fig. 6,7 shows the *interest points* detected on the head of the T-Rex and Parasaurolophus models using different numbers of scales in the scale-space representations.

The *interest points* in Fig.6 represent the more features that are extracted and the better than the geometric structures of the 3D triangular mesh models. In a high number of scales, we can demonstrate that *interest points* features such as the one on the embedded of the T-Rex model tooth and the parasaurolophus model lip can only be detected. The more scales used, the more number of *interest points* features can be detected. However, the computational time needed to establish these scales is more computationally expensive to these process with too many scales.

The spin images were selected features 201, 189, 105 and 114 for the Chef, Rhino, Angel and Zoe models as surface descriptors in order to perform 3D Registration with the *interest points* feature extraction proposed method. The proposed method produced more accurate results as the average registration errors were 1.980, 1.783, 1.232 and 1.345 compared to 1.901, 1.701, 1.129 and 1.318 as shown in Table II for the Chef, Rhino, Angel and Zoe models if using random points, respectively. Then, spin images are selected as surface descriptors in order to apply 3D surface registration using the proposed *interest points* feature extraction.

The pairwise registration as shown in Fig.8 represent to register two different views and the correspondences of these features were searched through all vertices of the other view to improve the probability of finding matches.

We combined the proposed *interest points* feature extraction and the spin image algorithm as local surface descriptors to register two different views of 3D object models. Fig.9 shows the accurate of pairwise registration for global registering 3D object models for three pairs of corresponding *interest points* features.

As illustrated in Table III and IV, the comparisons of translation and rotation errors between the spin image and the proposed method. They can be analyzed that the proposed method overcome the spin image approach in both the translation and rotation error metrics. Therefore, this proposed method a very suitable result for any global or coarse registration algorithm.

TABLE II  
COMPARISON OF THE REGISTRATION USING INTEREST POINTS FEATURE  
RANDOMLY AND LOCAL FEATURES FOR 4 MODELS

No.	Model	Registration using	Reg. time	Avg. error
1	Chef	Interest points randomly (6531)	3m14s	1.980
		Local shape features (201)	55s	1.901
2	Rhino	Interest points randomly (5674)	3m04s	1.783
		Local shape features (189)	47s	1.701
3	Angel	Interest points randomly (4073)	2m14s	1.232
		Local shape features (105)	50s	1.129
4	Zoe	Interest points randomly (4809)	2m46s	1.345
		Local shape features (114)	45s	1.318

TABLE III  
COMPARISON OF THE TRANSLATION ERRORS FOR 4 MODELS

No.	Model	Method	transl.-x	transl.-y	transl.-z
1	Chef	Spin Image	3.33	35.56	121.38
		The Proposed	2.24	7.69	17.85
2	Rhino	Spin Image	11.67	34.77	22.89
		The Proposed	1.57	2.45	1.56
3	Angel	Spin Image	4.44	21.67	22.67
		The Proposed	3.56	16.89	16.85
4	Zoe	Spin Image	5.85	1.46	1.28
		The Proposed	4.24	1.45	1.28

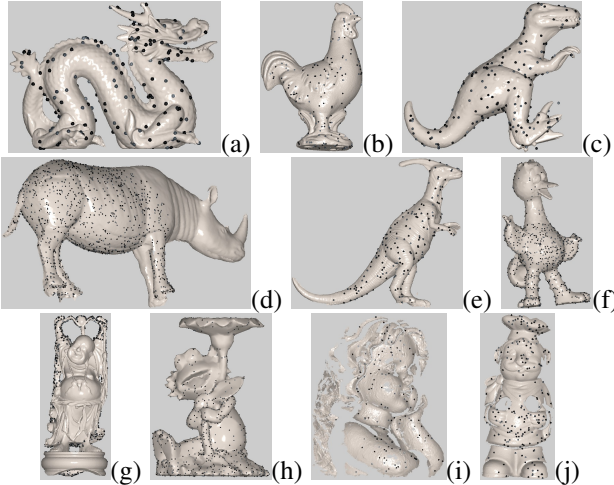


Fig. 3. Feature extraction results for tens different 3D models (a)Dragon (b) Chicken (c) T-rex (d) Rhino (e) Parasaurolophus (f) Bigbird (g) Buddha (h) Zoe (i) Angel view (h) chef view

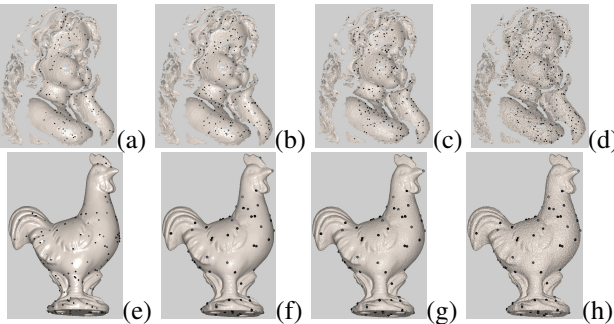


Fig. 4. *Interest points* features detected from the Chicken and Angel view models with different noise levels, a and e  $\sigma = 0$  (Original), b and f  $\sigma = 0.01$ , c and g  $\sigma = 0.1$ , and d and h  $\sigma = 0.2$

## VIII. CONCLUSION

In this paper, a framework for *interest points* extracting local features for 3D Triangular mesh based barycentric coordinates and global registering 3D object models for three pairs of corresponding *interest points* features have been presented. Initial experiments on a number of different standard triangular meshes described that the approach could robustly detect and localize local features from surfaces. The result of experiments clearly demonstrates it is more efficient and useful. The High repeatability of the points features and accurate pairwise registration. In our future work, we will develop this *interest points* local feature extraction framework and the proposed registration methods into some 3D object recognition.

## ACKNOWLEDGMENT

We would like to acknowledge: A.S. Mian dataset from the University of Western Australia, B. Taati Queen's Range Image and 3-D Model Database from Queen university and the Stanford Computer Graphics Laboratory for providing 3D model range data. This research is sponsored by Indonesian Government Scholarship (DIKTI-DIKNAS-RI)

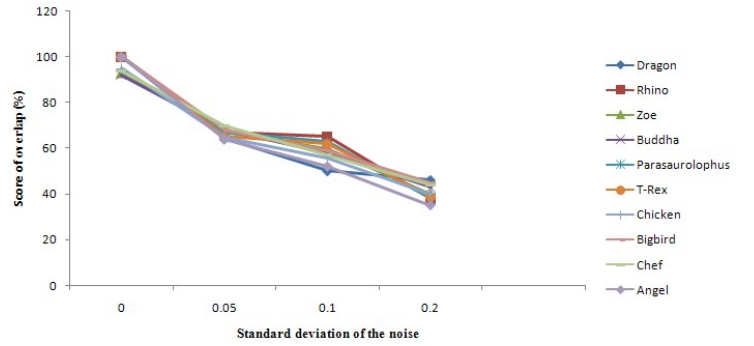


Fig. 5. Repeatability of the *Interest points* features ten different triangular mesh models using Barycentric Coordinates in noisy conditions

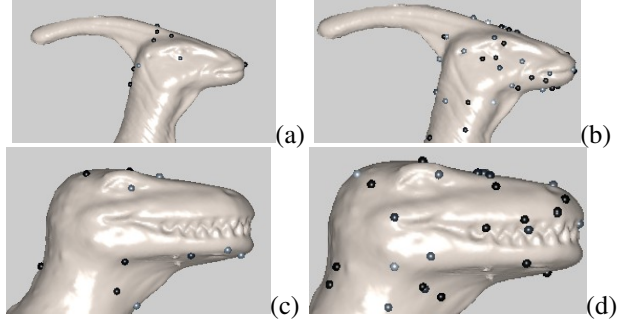


Fig. 6. *Interest points* features detected on the head of the T-Rex and parasaurolophus models at two scales for (a)and (c), four scales for (b)and (d)

## REFERENCES

- [1] A. Johnson and M. Hebert, "Using Spin Images for Efficient Object Recognition in Cluttered 3D Scenes," IEEE transactions on Pattern Analysis and Machine Intelligence, vol. 14, no. 5, pp. 674-686, May 1999.
- [2] A.S. Mian, M. Bennamoun and R. Owens, "A Novel Representation and Feature Matching Algorithm for Automatic Pairwise Registration of Range Images," International Journal of Computer Vision (IJCV), Copyright Springer Verlag, vol. 66(1), pp. 19-40, 2006.
- [3] A.S. Mian, M. Bennamoun and R. Owens, "3D Model-based Object Recognition and Segmentation in Cluttered Scenes," IEEE Transactions in Pattern Analysis and Machine Intelligence (IEEE TPAMI), . Copyright IEEE., vol. 28(10), pp. 1584-1601, 2006.
- [4] H. Dutagaci, C.P. Cheung and A. Godil "Evaluation 3D Interest Point Detection Techniques," Eurographics workshop on 3D Object Retrieval, 2011.
- [5] Castellani U., Cristani M., Fantoni S., and Murino V. "Sparse points matching by combining 3D mesh saliency with statistical descriptors," Computer Graphics Forum, vol. 27, pp. 643-652.2008.
- [6] A. Frome, D. Huber, R. Kolluri, T. Bulow, and J. Malik. "Recognizing Objects in Range Data using Regional Point Descriptors," In Proc. European Conf. Computer Vision, May 2004.
- [7] Toldo R., Castellani U. and Fusello A. "Visual vocabulary signature for 3D object retrieval and partial matching," In Proc. Eurographics Workshop on 3D Object Retrieval, 2009.
- [8] Harris C., and Stephens M., "A Combined corner and edge detection," In Proceedings of Fourth Alvey Vision Conference, Manchester-UK, pp. 147-151, 1988.
- [9] Sipiran I. and Bustos B., "A Robust 3D *interest points* detector Based on Harris Operator," Eurographics Workshop on 3D Object Retrieval, 2010.
- [10] B. Taati, M. Bondy, P. Jasbedzki, and M. Greenspan, "Variable Dimensional Local Shape Descriptors for Object Recognition in Range Data", Proceedings of the International Conference on Computer Vision (ICCV 2007) - 3D Representation for Recognition (3dRR), October 2007.

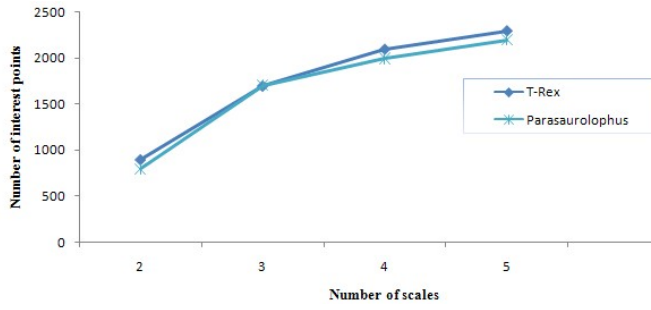


Fig. 7. Number of *interest points* features detected at various of scales

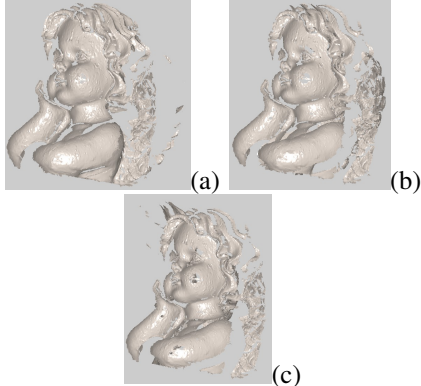


Fig. 8. Registration for 4 different views of Angel model.(a) Angel view 1 to 2 (b) Angel view 1 to 3 and (c) Angel view 1 to 4

- [11] "Queen's Range Image and 3-D Model Database," <http://rcvlab.ece.queensu.ca/qridb/QR3D/DatabasePagexyz.html>, 2009.
- [12] "The Stanford 3D Scanning Repository," <http://graphics.stanford.edu/data/3Dscanrep/>, Last modified 22 December 2010.
- [13] "Ajmal S. Mian dataset website," <http://www.csse.uwa.edu.au/ajmal/3Dmodeling.html>. 2006.
- [14] H.T. Ho, and D. Gibbons, "Curvature-based approach for multi-scale feature extraction from 3D meshes and unstructured point clouds," IET Computer Vision, Australia, volume 3, issue 4, pp. 201-142, 2009.
- [15] Dugopolski, M., Intermediate Algebra 3/e, McGrahill-Companies, USA, pp. 237-244, 2001.
- [16] R.M. Rustamov, "Barycentric Coordinates on Surfaces," Eurographics Symposium on Geometry Processing, number 5, volume 29, pp. 1-10, 2010.
- [17] Zhou Z.D., Ai Q.S., Liu Q., Yang L., Xie S.Q., and Chen Y.H., "A Novel Feature Points Selection Algorithm for 3D Triangular Mesh Models," ICSP2008 Proceedings, 2008.
- [18] Rohr, K., "Recognizing corners by fitting parametric models," Int. J. Comput. Vis., 9,(3), pp. 213-230, 1992.
- [19] Deriche, R., and Giraudon, G., "A computational approach for corner and vertex detection," Int. J. Comput. Vis., 10,(2), pp. 101-124, 1993.
- [20] Bottema, O. "On the Area of a Triangle in Barycentric Coordinates." Crux. Math. 8, 228-231, 1982.
- [21] Coxeter, H. S. M. "Barycentric Coordinates." 13.7 in Introduction to Geometry, 2nd ed. New York: Wiley, pp. 216-221, 1969.
- [22] K.Mikolajczyk and C.Schmid. "Indexing Based on Scale Invariant Interest Points.", Proceedings of Eighth IEEE International Conference on Computer Vision, Vol. 1, pp. 525-531, 2001.
- [23] S. Rusinkiewics and M. Levoy. "Efficient Variants of the ICP Algorithm" In Proceeding 3DIM, pages 145-152, 2001.
- [24] O. Carmichael, D. Huber and M. Hebert. "3D Cueing : A Data Filter For Object Recognition", Proceedings of IEEE International Conference on Robotics and Automation (ICRA '99), pp. 944 - 950, May, 1999.
- [25] O. Carmichael, D. Huber and M. Hebert. "Large Data Sets and Con-

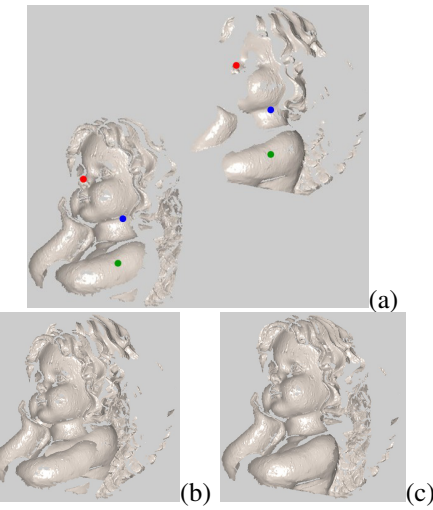


Fig. 9. Pairwise Registration results for the Angel model.(a) Angel view 1 and 2 (b) Spin image result and (c)The proposed result

TABLE IV  
COMPARISON OF THE ROTATION ERRORS FOR 4 MODELS

No.	Model	Method	rot.-x(o)	rot.-y(o)	rot.-z(o)
1	Chef	Spin Image	25.83	3.46	3.87
		The Proposed	0.75	0.92	2.81
2	Rhino	Spin Image	8.12	4.34	8.09
		The Proposed	0.65	0.72	1.01
3	Angel	Spin Image	4.01	0.78	0.85
		The Proposed	0.67	0.49	0.78
4	Zoe	Spin Image	0.94	3.12	2.76
		The Proposed	0.41	2.23	0.94

- fusing Scenes in 3-D surface Matching and Recognition", Proceedings of the Second International Conference on 3-D Digital Imaging and Modeling (3DIM'99), pp. 358-367, October, 1999.
- [26] H. Dinh and S. Kropac. "Multi-Resolution Spin-Images", Proceedings of the 2006 IEEE Computer Society Conference on Computer Vision and Pattern Recognition, Volume: 1, Publisher: IEEE Computer Society, pp. 863-870, June, 2006.
- [27] O. Stasse, S. Duplifter and K. Yokoi. "3D object recognition using spin-images for a humanoid stereoscopic vision system", Proceedings of the 2006 IEEE International Conference on Intelligent Robots and Systems, Beijing, China, October 9 - 15, 2006.
- [28] S. Ruiz-Correa, L.G. Shapiro, and M.; Melia. "A new signature-based method for efficient 3-D object recognition", Proceedings of the 2001 IEEE Computer Society Conference on Computer Vision and Pattern Recognition, Washington Univ., Seattle, WA, USA, pages. I-769 - I-776, vol.1, 2001.
- [29] A. Halma, F. Haar, E. Bovenkamp and P. Eendebak. "Single spin image-ICP matching for efficient 3D object recognition", Proceedings of the ACM workshop on 3D object retrieval, ACM New York, NY, USA, pp. 21-26, 2010.
- [30] T. Tamaki, S. Tanigawa, Y. Ueno and B. Raytchev and K. Kaneda. "Scale Matching of 3D Point Clouds by Finding Keyscales with Spin Images", Proceedings of the 2010 20th International Conference on Pattern Recognition, IEEE Computer Society Washington, DC, USA, pp. 3480-3483, 2010.
- [31] C. Matabosch, J. Salvi, D. Fofi and F. Meriaudeau. "Range Image Registration for Industrial Inspection", Proceedings of the Machine Vision Applications in Industrial Inspection XIII MVAII 05, San Jose, California, USA, January 16-20, 2005
- [32] G. Roth. "Registering Two Overlapping Range Images". Proceedings of 3DIM, pp. 191-200, 1999.